Screening Procedure for Synthesizing Isothermal Multiphase Reactors

Vaibhav V. Kelkar and Ka M. Ng
Dept. of Chemical Engineering, University of Massachusetts, Amherst, MA 01003

A procedure is developed to identify a multiphase reactor for carrying out a given reaction at the early stage of process development. There are three elements to this screening approach: a generic reactor model, an accompanying sensitivity model, and a knowledge base consisting of heuristics, plus correlations on hydrodynamics, heat, and mass transport. In synthesizing a generic reactor model, the conventional multiphase reactors are decomposed into common attributes and constituent parts, and reaggregated for the reaction under consideration. Thus, in addition to choosing one among conventional reactor types, the procedure provides insights for the creation of novel reactors. The sensitivity model quantifies the relative impact of the model parameters on the reactor performance. The knowledge base provides heuristics, estimates, and reality checks in the decision-making process. While this article focuses on isothermal systems with a single reaction, the framework is applicable for general multiphase reactions.

Introduction

Gas–liquid and liquid–liquid reactions with or without the presence of a solid catalyst provide the basis for a large number of chemical, petrochemical, and biochemical operations. Examples include oxidation, hydrogenation, hydroformylation, amination, and carbonylation. A wide variety of multiphase reactors are used for such multiphase reactions, including agitated reactors, bubble columns, trickle-bed reactors, spray columns, and jet loop reactors. There is considerable information in the literature about the analysis and design of multiphase reactors, including several notable texts and monographs (Shah, 1979, 1991; Ramachandran and Chaudhari, 1983; Doraiswamy and Sharma, 1984; Gianetto and Silveston, 1986; Mills et al., 1992).

When the chemist proposes a multiphase reaction for possible commercialization, a reactor type needs to be chosen for further process development. Reactor selection is normally based on the use of heuristics and expert insights. For example, Mills et al. (1992) provide a comprehensive description of the characteristics, advantages, and disadvantages of various multiphase reactor types. Then, the design of the chosen reactor proceeds with detailed reactor modeling, taking into account the hydrodynamics, heat, and mass transfer as well as the reaction kinetics. This is accompanied by scale-up efforts to confirm reactor performance and to provide basic data for the commercial reactor. Early commitment to a specific reactor type is deemed necessary because of the substantial development costs.

As a better understanding of the reaction system evolves with time, however, it is not unusual to find out that the commercial reactor on the ground was not the best selection and is inflicting considerable economic penalty on a continuous basis. For an interesting account of the evolution of the nitric acid reactor in an adipic acid plant, see Hearfield (1980). Thus, the availability of tools and/or systematic procedures for more efficient screening of multiphase reactors is highly desirable (Lerou and Ng, 1996). An effort in this direction is due to Krishna and Sie (1994), who proposed a strategy for multiphase reactor selection. It consists of three levels: catalyst design, injection and dispersion strategy, and choice of hydrodynamic flow regime. In contrast, a more conventional approach was adopted by Schembecker et al. (1995); models for various reactor types are encoded in a computer program as an aid for reactor selection and design. More recently, Mehta and Kokossis (1997) proposed modeling a multiphase reactor as a network of idealized reactors. For a given reaction scheme and kinetics, optimization using simulated annealing leads to a reactor type that is optimal with respect to a specified objective function.

Correspondence concerning this article should be addressed to K. M. Ng.

As an alternative approach to these previous studies, the objective of this article is to develop a semiquantitative procedure/framework for synthesizing a multiphase reactor, focusing on the early stage of reactor development. The proposed reaction is still being investigated by the chemist with various laboratory reactors, including microreactors and bench-scale reactors that can be completely different from the eventual commercial reactor. Special emphasis is placed on situations where there is a great deal of uncertainty regarding reaction kinetics, and little is known about potential limitations in heat and mass transfer.

One element of our framework is a generic multiphase reactor model. Its formulation is based on the realization that despite the considerable differences in phase distribution, multiphase reactors can be compared on the basis of common attributes such as phase volumes, phase velocities, and various transport parameters. Multiphase reactors also share reactor parts such as a liquid mixer, baffles, and a gas sparger. These constituent parts are abstracted into the generic multiphase reactor model. In other words, conventional multiphase reactors are decomposed into common attributes and constituent parts, and reaggregated for the specific reaction under consideration. Not only can the model represent the conventional reactor types, but it is also expected to provide insights for the use of unconventional reactors. The second element is a companion sensitivity model to the reactor

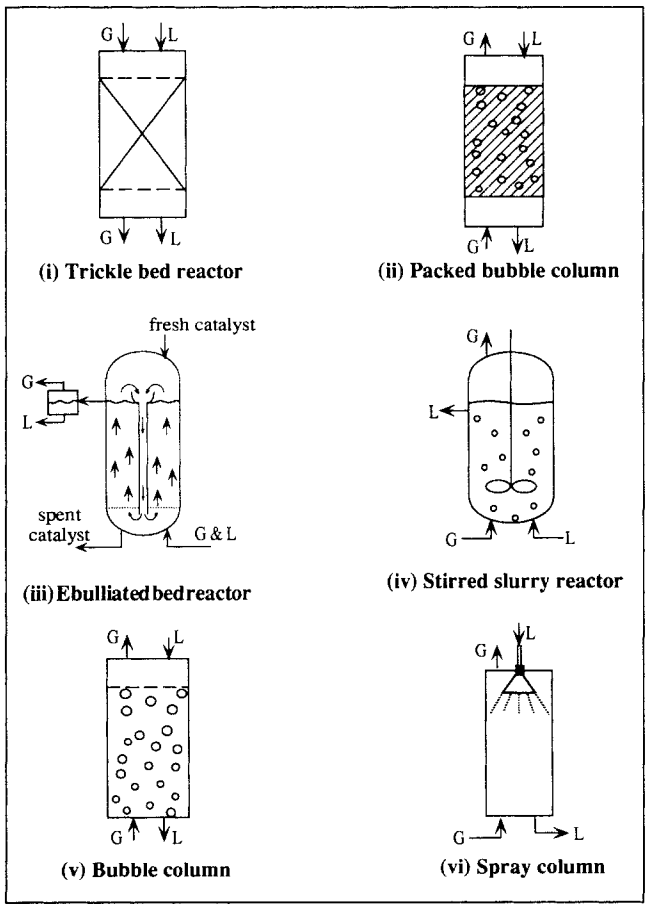

Figure 1a. Selected multiphase reactors for gas–liquid, gas–liquid–catalytic solid and liquid–liquid reactions.

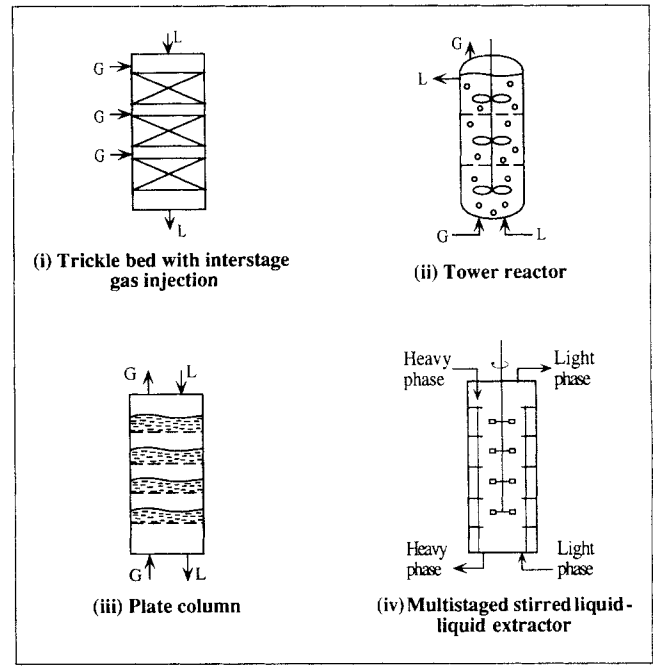

Figure 1b. Selected multiphase reactors with physical compartmentalization.

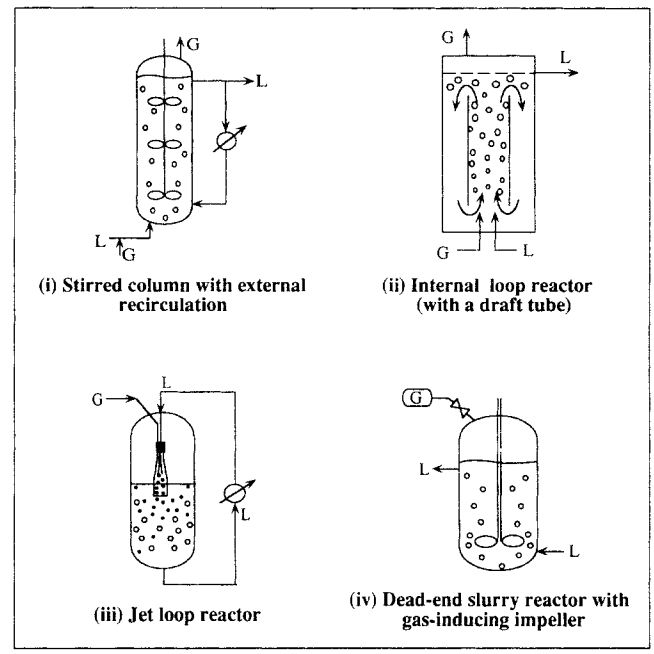

Figure 1c. Selected multiphase reactors having internal or external recirculation of phases.

model. By screening the sensitivity of reactor performance to each of the reactor characteristics as well as to the still-uncertain kinetic and thermodynamic parameters, the dominant factor dictating the reactor performance, such as the reaction rate, interfacial area, or mass-transfer rate, is identified. The third element is a knowledge base that includes heuristics, flow-regime characteristics, correlations for heat and mass transfer, and others; it is used in this procedure to guide the decision-making process. While the framework is valid for general multiphase reactions, because of the enor-

mous number of details involved, the present article focuses primarily on isothermal, nonfoaming systems with a single reaction.

Generic View of Multiphase Reactors

Our generic multiphase reactor model is predicated on an identification of four classes of common features among the seemingly different multiphase reactors. Due to the interrelationships among the various features in a multiphase reactor, however, a minor overlap in the classification is inevitable. To facilitate the discussion, some typical multiphase reactors for gas–liquid, gas–liquid–catalytic solid, and liquid–liquid applications are depicted in Figure 1a. Reactor types with compartments and phase recirculations are shown in Figures 1b and 1c, respectively. Within each subset (Figures 1a, 1b, and 1c) the reactors are ordered with a roughly decreasing amount of solid in the reactor.

Phase-distribution attributes

Clearly, a major reason for having all these different reactor types is the variety of ways in which gas, liquid, and solid are distributed in the reactor. For example, Figure 1a shows some multiphase reactors having a wide range of phase distributions. Despite the diversity, the following common attributes can be used to define the state of each phase:

- Is the phase fixed, recirculating within, or passing through the reactor?
- Which phase is continuous and which is dispersed?
- What is the physical form of each phase? Is it films, bubbles, drops, or simply a continuum?

More quantitative descriptions include:

- What is the flow rate of each phase?
- What is the volume fraction of each phase?
- What is the interfacial area between the phases?
- What is the size distribution of the bubbles and drops?
- What is the state of mixedness of each phase: plug, dispersed, or well mixed?

As part of our knowledge base on phase distribution, Figure 2 shows the generic *volume fraction map* for each phase. Each phase is classified as being *dispersed*, *fluidized*, *packed*, or *continuous* as the corresponding volume fraction increases. The range of the dispersed solid volume fraction, ϵ_S, corresponds to a slurry reactor, either a bubble column or an agitated tank, while the packed solid fraction range corresponds to that of a trickle-bed reactor. The catalyst particle size in each volume fraction range is different, and typical values are given in the following table:

	Dispersed (Sparged)	Dispersed (Stirred)	Fluidized	Packed
d_p	10–100 μm	10–200 μm	0.01–0.1 cm	0.3–0.5 cm

The size is relatively small in the dispersed state because of the need for suspending the particles. In the packed state, the smallest particle size is determined by the presence of excessive pressure drop. Note that the shadings used for ϵ_G and ϵ_L correspond to the state of the solid phase. For the

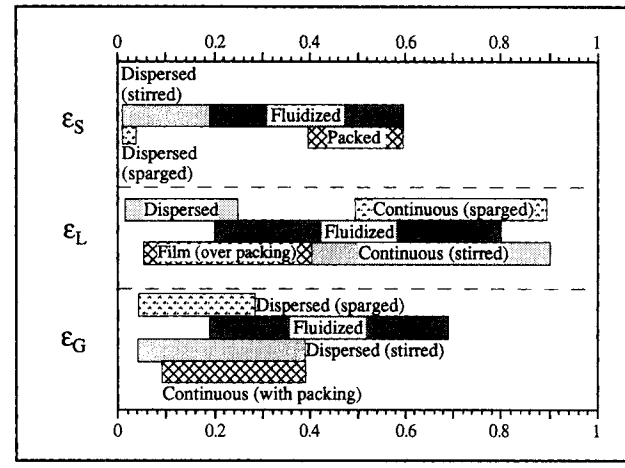

Figure 2. Generic phase volume fraction map for gas, liquid, and solid phases.

liquid phase in a dispersed state, such as in a spray-column reactor, the liquid volume fraction, ϵ_L, ranges from 0.02 to 0.2, whereas in a continuous state as in a bubble column ϵ_L ranges from about 0.6 to 0.9. It is clear from this map that for situations where an equal volume fraction of gas, liquid, and solid is preferred, the fluidized state is the obvious choice. The volume fraction also depends on the flow regime. Figure 3 shows the *holdup-flow regime maps* for the dispersed (slurry

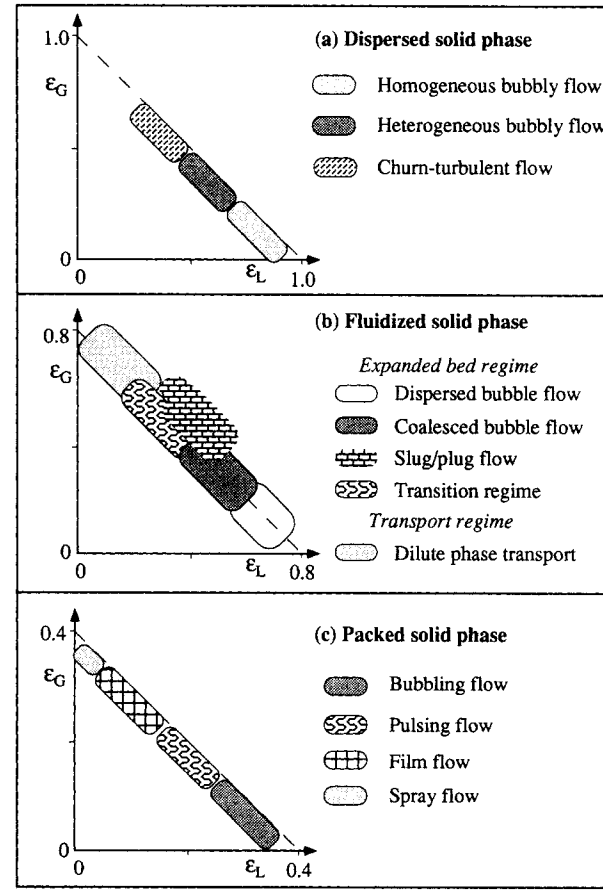

Figure 3. Holdup flow regime for conventional reactors.

bubble column), fluidized (three-phase fluid bed), and packed (trickle-bed) state of the solid phase. Thus, it is possible to identify both the reactor type as well as the flow regime for a set of desired phase-volume fractions. In turn, the dependency of the flow regime on the gas and liquid flow rates can be obtained from the conventional *flow-regime maps*. For example, see Ramachandran and Chaudhari (1983) for such maps for bubble columns; Fan (1989) and Bi and Grace (1995) for that of fluidized beds; Ng (1986) and Ng and Chu (1994) for that of a trickle-bed reactor. Some heuristics for selecting solid phase volume fraction are presented below for the dispersed, fluidized, or packed states:

Dispersed

- Systems with a higher reaction rate relative to intraparticle diffusion rate.
- Systems with reaction kinetics favoring completely mixed flow patterns.
- Highly exothermic reactions.
- Systems requiring a continuous addition or removal of catalyst.
- Systems that require isothermal operation.
- Treating a feed with a small amount of extraneous inert solids.
- Treating a feed with solid reactants.
- Operations requiring a flexibility between batch/semibatch/continuous modes.

Fluidized

- Systems comprising approximately equal amounts of gas, liquid, and solids.
- Systems requiring a continuous addition or removal of catalyst, for example, rapidly deactivating catalysts.
- Systems with reaction kinetics favoring completely mixed flow patterns.
- Systems that require isothermal operation.

Packed

- Systems with a low reaction rate relative to the intraparticle diffusion rate, that is, when a high catalyst loading is required to get a high specific reaction rate.
- Systems with reaction kinetics favoring plug-flow patterns.
- Systems with homogeneous side reactions in the liquid phase.
- Catalysts that do not deactivate rapidly.
- Systems where catalyst loss has to be minimized.

Other phase-distribution attributes include the gas–liquid, liquid–liquid, and liquid–solid interfacial areas, which influence the rates of interphase mass transfer and interfacial reactions. However, because of the close association between interfacial area and the corresponding mass-transfer coefficients, they will be treated together in a later section.

Reactor topological/geometrical characteristics

In addition to phase distribution, the designer can also manipulate various reactor geometrical characteristics, which include:

- What is the relative motion of the phases: cocurrent, countercurrent, or crossflow?
- What is the overall shape of the reactor, such as its aspect ratio?
- Is the reactor compartmentalized by various physical partitions? Figure 1b shows multiphase reactors with some form of physical compartmentalization.
- What is the extent of partitioning? The horizontal partitions in a tower reactor (Figure 1b(ii)) can be sufficiently large that the intermixing between the chambers can be significantly reduced. In contrast, the relatively small vertical baffles in an agitated slurry reactor promote mixing of the phases.
- Is there a recirculation of the phases, either internally (e.g., draft tube) or externally (e.g., external loop), of the reactor? Note that phase recirculation can be induced by impellers or a jet mixer alone without the presence of partitions. A few reactors that involve internal or external recirculation of phases are depicted in Figure 1c.
- What are the number of feed and removal ports? Where are they located?

Figure 4 shows how these characteristics are abstracted into various geometrical representations. Figure 4a shows a countercurrent solid–catalytic reactor with single feed and removal ports. Note that it can represent either a dispersed, fluidized, or packed reactor, depending on the solid phase volume. Figure 4b shows a representation of a reactor where a phase is recirculated, either internally or externally. Figure 4c shows vertical compartmentalization, whereas Figure 4d shows a bank of parallel units. Figure 4e is a reactor of a low

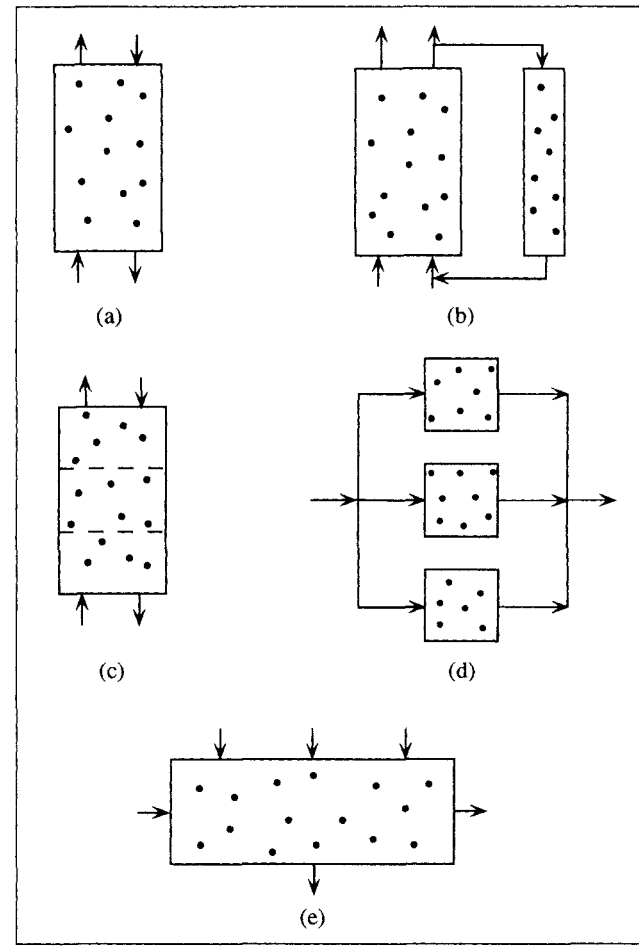

Figure 4. Reactor geometrical and topological characteristics.

aspect ratio. Some of the heuristics for selecting various reactor geometrical characteristics are presented below:

- Use impellers at high rpm to enhance the mass-transfer rate by up to a factor of 5.
- Use propellers to enhance solids suspension.
- Use vigorous mixing with impellers to enhance the heat-transfer coefficient by up to a factor of 10 at the wall of a stirred tank.
- Use a downward pumping propeller to enhance gas absorption.
- Use gas-inducing impellers to recirculate the unreacted gaseous reactant.
- Use multiple sets of impellers on a single shaft to enhance the uniformity of mixing in a large-scale reactor.
- Use a tilted or off-centered impeller shaft to improve mixing in the absence of vertical baffles.
- Use a venturi ejector for fast, mass-transfer limited reactions.
- Use multiple nozzles to enhance gas absorption.
- Use horizontal baffles along a vertical reactor to reduce backmixing.
- Use vertical baffles to enhance mixing by reducing solid-body rotation.
- Use draft tubes to induce internal recirculation of the liquid.
- Use internal heating or cooling coils for reactor heat management.

Reactor constituent parts

Many attributes of phase distribution are determined by distinct parts of the reactor. *Gas–liquid interface generating device:* Some of the devices can be found in Figure 1: an impeller for a stirred reactor (Figure 1a(iv)), a gas sparger in a bubble column (Figure 1a(v)), a liquid spray (Figure 1a(vi)), a venturi ejector (Figure 1c(iii)), and a gas-inducing impeller (Figure 1c(iv)). *Gas recirculation device:* Gas-inducing impellers (Figure 1c(iii)) and downflow impellers can be used for internal recirculation. The latter device has been successfully used for improving the performance of oxidation reactors (Kingsley and Roby, 1996). External recirculation can be accomplished by using a compressor and an external loop.

Liquid mixing and recirculation device: This is powered by the different impellers and propellers, a liquid jet (which is in turn powered by a pump), or gas flow as in the gas-lift reactor or the bubble column. These devices, as their gas counterparts, are used in combination with the partitions described earlier to maximize their effectiveness. *Solid-phase structure:* The solid phase could be catalytic in nature or simply an inert packing for generating a gas–liquid interface. It can be in the form of small spherical particles or cylindrical extrudates, or structured packings such as trilobes and wagon wheels. More recently, structured monolith reactors with thin liquid films have been proposed to provide reaction rates close to their intrinsic values (Cybulski and Moulijn, 1994).

Heuristics for choosing various reactor constituent parts are:

- Use countercurrent contacting for a mass-transfer-controlled reaction where a high concentration driving force is essential.
- To avoid flooding, use cocurrent downflow for systems with high gas and liquid throughputs.
- Use cocurrent upflow to save compressor cost; however, use cocurrent downflow if gas dispersion has an adverse effect on conversion.
- Use interstage injection of cold reactants to prevent hot spots with highly exothermic reactions.
- Use plug flow for reactions with a high reaction order.
- Use mixed flow for reactions with a low reaction order and reactions requiring isothermal operations.
- Use internal recirculation loop when macroscopic liquid recirculation at low energy input is desirable and when high shear rates during liquid mixing are undesirable, for example, in the case of biological systems.
- Use an external loop for highly exothermic reactions that require external heat removal.
- Use an external loop to enhance gas absorption.
- Use liquid redistributors to compartmentalize a trickle-bed reactor to reduce channeling effect in trickle-bed reactors.
- Use compartments along the reactor to reduce backmixing.
- Use compartments to allow interstage injection of a reactant to improve selectivity.
- Use multiple-tube reactors to enhance heat removal and to minimize radial temperature gradients.

Transport and thermodynamic parameters

Regardless of the differences in phase distribution, multiphase reactors may share various transport parameters, such as gas–liquid, liquid–liquid, and liquid–solid mass-transfer coefficients, and thermodynamic parameters, such as solubility and Henry's law constant. Some reactor parameters and phase distribution attributes, such as the gas–liquid interfacial area in different multiphase reactors, are not a property of the reactors themselves, but primarily of the constituent part generating the parameter value. Applying this approach to recast the existing information so as to reflect the role of different constituent parts yields the *Generic Transport Parameters Maps* (Figure 5). Figure 5a shows the range of gas–liquid interfacial area and the corresponding mass-transfer coefficient for various gas–liquid interface generating devices. For example, the gas–liquid interfacial area can range from about 100 m^{-1} to 400 m^{-1} for a liquid film in a packed bed, whereas it can be as high as 1,800 m^{-1} using a gas sparger, and even higher with a jet mixer. Figure 5b shows the range of solid surface area as well as the corresponding range for the liquid–solid mass-transfer coefficient for various states of the solid phase.

Generic Multiphase Reactor Model

In this synthesis procedure, the purpose of the reactor model is not to simulate the reactors in detail. Rather, it serves as a tool for differentiating between different reactor types based on the values of reactor parameters, phase distribution, macroscopic mixing patterns in all three phases, and the geometry of the reactor. This objective can be met with a model made up of a network of reactors such as perfectly mixed stirred tanks, plug flow tubes, and plug flow with dispersion vessels. Because of their computational convenience,

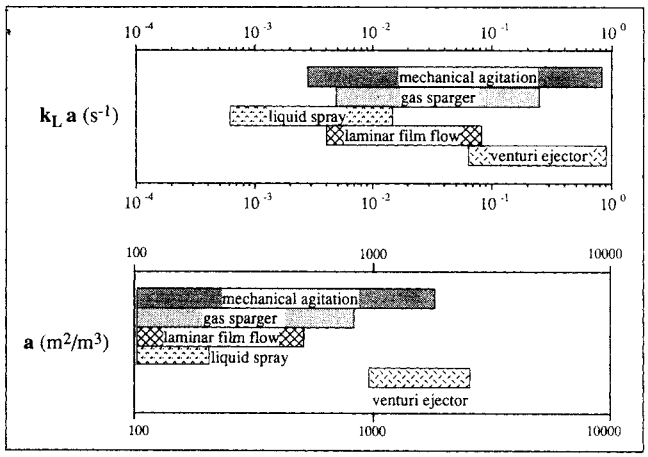

Figure 5a. Gas–liquid interfacial area and mass-transfer coefficients for various interface generating devices.

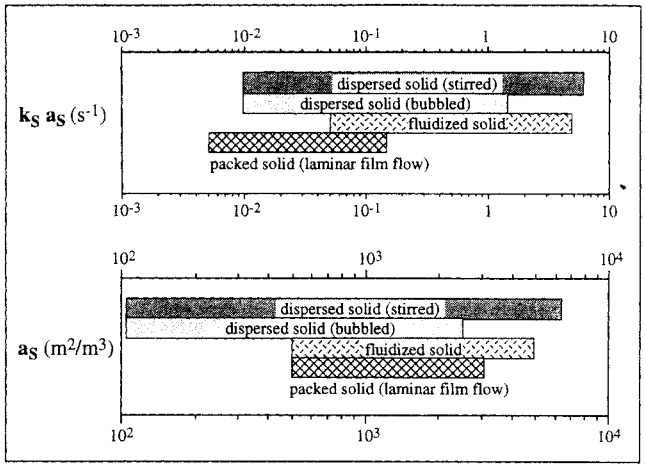

Figure 5b. Liquid–solid interfacial area and mass-transfer coefficients for various states of the solid phase.

network models are very popular. For example, a network of stirred tanks has been used to represent a single agitated tank (Mann, 1986) as well as a trickle-bed reactor (Ramachandran and Smith, 1979). Earlier network models have been reviewed in the monograph by Wen and Fan (1975). Rather than using a network to represent a single reactor, the synthesis of a network of multiple physically distinct reactors for improving yield and selectivity has also been extensively investigated (Kokossis and Floudas, 1990, 1994; Hildebrandt and Glasser, 1990; Hildebrandt and Biegler, 1994).

Figure 6 shows a few example networks for cases where the solid phase is either absent or remains within the reactor. Figures 6a, 6b, and 6c are the three basic units, to be referred to as cells of the network. Figure 6d shows a three-cell network with interstage gas injection. Figure 6e represents a reactor where both the gas and liquid are recirculated. By adjusting the recirculation ratios, the mixedness of the gas and liquid phases can be varied over a wide range, from relatively plug flow to relatively well mixed. Figure 6f shows a bank of parallel stirred tanks, and can represent a reactor

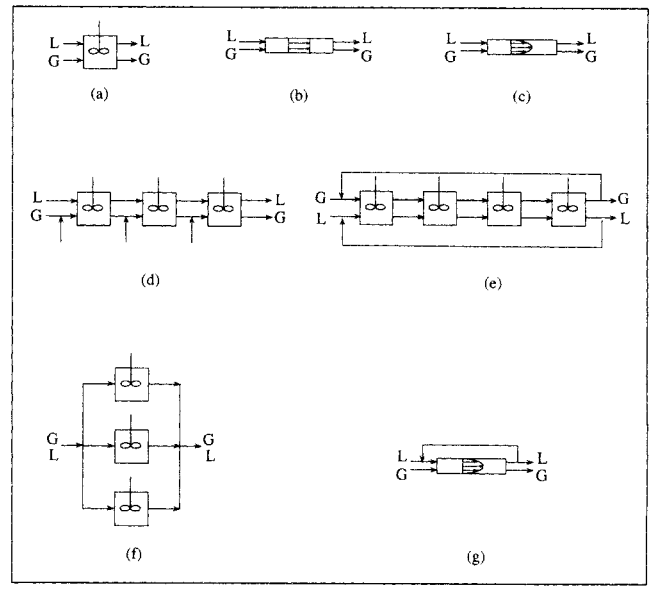

Figure 6. Examples of network models.

with a low aspect ratio. An axial dispersion reactor with recycle for the liquid is shown in Figure 6g (cf. Figure 4b). The heuristics for selecting various reactor geometrical characteristics listed earlier can be used for selecting networks for screening calculations. The models should be made as simple as possible initially. The use of elaborate networks, in terms of the network size and the interconnections between the individual cells, should be considered if the complexity is commensurate with the accuracy of other reactor parameters and reaction kinetics.

In this article, we focus on a general-order irreversible gas–liquid, liquid–liquid, or gas–liquid–solid catalytic reaction of the following form:

$$\sum_i \nu_i A_i = 0. \tag{1}$$

The kinetics can be represented by power law, Langmuir–Hinshelwood kinetics, or other rate expressions. Assuming that some basic information is known about this reaction, our task is to synthesize alternative reactor types that are appropriate for the reaction under consideration. Once the interconnection of the cells in the network has been made, the set of equations for simulating such a network can be compiled using standard equations for a stirred tank, plug flow, or a plug flow with dispersion model, as well as the material balance equations at each mixing point in the network. Thus, a steady-state reacting system can be described by the following general equation:

$$f\left(\frac{d^2c}{dz^2}, \frac{dc}{dz}, c;\ z, \boldsymbol{\alpha}, \boldsymbol{\beta}\right) = \mathbf{0}, \tag{2}$$

with the appropriate boundary conditions. Here, $\boldsymbol{c}$ is the vector of concentrations of all the species in all the phases, $\boldsymbol{\alpha}$ is the vector of phase distribution attributes such as ϵ_G, ϵ_L, ϵ_S, a, and a_S, and $\boldsymbol{\beta}$ is the set of transport and thermodynamic

parameters such as $k_L a$, H, and D_e. Note that depending on the structure of the model chosen, the general equation can be greatly simplified. For example, for a network represented with only stirred tanks, the derivative terms are absent. Equation 2 becomes

$$f(c;\ \alpha,\ \beta) = 0. \tag{3}$$

Sensitivity models

A sensitivity model accompanies each reactor model in order to quantify the relative impact of various variables—phase distribution attributes, transport, and thermodynamic parameters—on the performance of the reactor yet to be synthesized. A number of methods can be used for the sensitivity analysis (Rabitz et al., 1983). The finite difference method is conceptually the simplest. It calculates the sensitivity to a small change in α via difference approximations; see Rajagopal et al. (1988) for an example. Our sensitivity analysis is based on the direct differential method, which involves the solution of the sensitivity equations derived from Eq. 2. Differentiating Eq. 2 with respect to the phase parameter α_j gives

$$\left(\frac{\partial f}{\partial c''}\right)_{\alpha,\beta}\frac{d^2 s_j}{dz^2} + \left(\frac{\partial f}{\partial c'}\right)_{\alpha,\beta}\frac{ds_j}{dz} + \left(\frac{\partial f}{\partial c}\right)_{\alpha,\beta} s_j + \left(\frac{\partial f}{\partial \alpha_j}\right)_{\alpha_{i\neq j},c,\beta} = 0. \tag{4}$$

The vector of sensitivity coefficients s_j is defined as

$$s_j = \frac{\partial c}{\partial \alpha_j}. \tag{5}$$

Thus, each variable in the model has a sensitivity coefficient with respect to every parameter of interest. Note that the parameters α and β are mathematically equivalent; they only refer to different types of reactor parameters, as defined earlier. Although the transport parameters β may depend on the phase distribution parameters α for screening purposes, they can be treated as mathematically independent in the sensitivity analysis. Again, for the limiting case of stirred tanks only, we have

$$\left(\frac{\partial f}{\partial c}\right)_{\alpha,\beta} s_j + \frac{\partial f}{\partial \alpha_j} = 0. \tag{6}$$

Performance index

The sensitivity of the concentrations to the reactor parameters is not the most useful piece of information that can be obtained. Frequently, we are concerned with the sensitivity of some kind of performance index such as the conversion, selectivity, or the total cost to the reactor parameters. If the performance index can be written as a function of the reactor concentrations, the parameters α and β, and some other variables q,

$$P = P(c;\ \alpha,\ \beta,\ q), \tag{7}$$

then the sensitivity of the performance index, $\psi(\alpha_j)$, can be obtained as

$$\psi(\alpha_j) = \frac{\partial P}{\partial \alpha_j} = \left(\frac{\partial P}{\partial c}\right) s_j + \frac{\partial P}{\partial \alpha_j} + \left(\frac{\partial P}{\partial q}\right)\left(\frac{\partial q}{\partial \alpha_j}\right). \tag{8}$$

Here, q includes all the external variables required to relate the performance index to the concentrations, α and β. For example, if the performance index is taken to be the reactor cost, q would include parameters that reflect the costs of the materials of construction and auxiliary equipment for the reactor.

Normalized sensitivity coefficients

In general, the parameters α_i and β_i have different orders of magnitude; for example, the diffusion coefficient, D_e, is of the order of 10^{-6} cm^2/s, while the holdups, ϵ_S, ϵ_G, ϵ_L, are of the order unity. To compare them on an equal basis, the sensitivity coefficients $\psi(\alpha_i)$ have to be normalized as follows:

$$\bar{\psi}(\alpha_j) = \frac{\partial P}{\partial(\alpha_j/\Delta\alpha_{j,\max})} = \psi(\alpha_j)\Delta\alpha_{j,\max}, \tag{9}$$

where $\Delta\alpha_{j,\max}$ is the maximum expected range of α_j. The larger a normalized sensitivity coefficient, the more impact the corresponding parameter α_j exerts on the performance index.

Model illustration

Let us consider a network of N stirred tanks in series with recycles for a gas–liquid–solid catalyst reaction (Figure 6e). This model can represent the macroscopic mixing patterns for reactors ranging from a stirred tank on one extreme to a trickle bed on the other. It allows a recycle of gas as well as liquid, and hence the backmixing in the two phases can be varied independently. The rate of reaction per unit volume of reactor is given by

$$\text{Rate} = \eta_c w \Phi(C_i) \tag{10}$$

where the $\Phi(C_i)$ can be any given function of the concentrations, such as a power law, or Langmuir–Hinshelwood type of expression. There are m_G reactants present in the gas feed, and m_L nonvolatile reactants in the liquid feed. Gas-phase material balances for species i in the jth cell are as follows:

$$Q_G[G_i(j-1) - G_i(j)] - Vk_L a\left[\frac{G_i(j)}{H_i} - L_i(j)\right] = 0 \qquad i = 1, \ldots, m_G. \tag{11}$$

Here, $G_i(j)$ and $L_i(j)$ are the concentrations of species i in the gas and liquid phases, respectively. Liquid-phase material balances are

$$Vk_La\left[\frac{G_i(j)}{H_i}-L_i(j)\right]+Q_L[L_i(j-1)-L_i(j)]$$
$$-Vk_Sa_S[L_i(j)-S_i(j)]=0 \quad i=1,\ \ldots,\ m_G \quad (12a)$$

and

$$Q_L[L_i(j-1)-L_i(j)]-Vk_Sa_S[L_i(j)-S_i(j)]=0$$
$$i=m_G+1,\ \ldots,\ m_G+m_L. \quad (12b)$$

Here, $S_i(j)$ is the concentration of species i at the catalyst surface. Solid-phase material balances are

$$Vk_Sa_S[L_i(j)-S_i(j)]-V\eta_c w\Phi[\mathbf{S}(j)]=0$$
$$i=1,\ \ldots,\ m_G+m_L. \quad (13)$$

Since a portion of the gas and liquid phase may be recycled to the first cell, the concentrations at the inlet to the first cell [$G_i(0)$ and $L_i(0)$] are unknown. Two additional material balances are required at the inlet to the first cell, one for the gas phase and another for the liquid phase:

$$G_i(0)\left(\frac{F_G}{1-r_G}\right)=F_GG_i^f+G_i(N)F_G\left(\frac{r_G}{1-r_G}\right) \quad (14)$$

$$L_i(0)\left(\frac{F_L}{1-r_L}\right)=F_LL_i^f+L_i(N)F_L\left(\frac{r_L}{1-r_L}\right), \quad (15)$$

where F_G and F_L are the fresh feed volumetric flow rates of the gas and liquid phases, respectively. The recycle ratios r_G and r_L are defined as

$$r_G=\frac{Q_G-F_G}{Q_G} \quad \text{and} \quad r_L=\frac{Q_L-F_L}{Q_L}. \quad (16)$$

Following Bischoff (1965), the effectiveness factor η_c is approximated as

$$\eta_c=\frac{1}{\phi}\left(\frac{1}{\tanh 3\phi}-\frac{1}{3\phi}\right), \quad (17)$$

where ϕ is the generalized Thiele modulus given by

$$\phi=\frac{V_p}{S_p}\frac{\Phi[S_1(j)]}{\sqrt{2}}\left[\int_0^{S_1(j)}D_l\Phi(C_1)\,dC_1\right]^{1/2} \quad (18)$$

where species l is assumed to be the limiting reactant on the catalyst surface. For a spherical catalyst, and a reaction first order in species l and independent of all others, the preceding expression simplifies to

$$\phi=\frac{d_p}{6}\sqrt{\frac{k\mathrm{P}_p}{D_l}}. \quad (19)$$

Equations 11–15 form a set of $(3m_G+2m_L)N+(2m_G+m_L)$ nonlinear algebraic equations in the same number of unknowns. The unknowns are the concentrations of all m_G+m_L species in the gas, liquid, and catalyst phases, in each of the N cells, as well as the concentrations in the gas and liquid phase at the inlet to the first cell. Note that the liquid reactants are considered to be nonvolatile, so they are not present in the gas phase.

Sensitivity model

The parameters that we might like to consider are k_La, k_Sa_S, k, d_p, w, D_e, and the effectiveness factor η_c. The sensitivity equations are obtained by differentiating the model equations (Eqs. 11 through 15) with respect to the parameter of interest. For example, with k_La as parameter, the sensitivity equations are as follows:

Gas Phase

$$Q_G\left[s_i^G(j-1)-s_i^G(j)\right]-Vk_La\left[\frac{s_i^G(j)}{H_i}-s_i^L(j)\right]$$
$$-V\left[\frac{G_i(j)}{H_i}-L_i(j)\right]=0. \quad (20)$$

Liquid Phase

$$Vk_La\left[\frac{s_i^G(j)}{H_i}-s_i^L(j)\right]+V\left[\frac{G_i(j)}{H_i}-L_i(j)\right]$$
$$+Q_L\left[s_i^L(j-1)-s_i^L(j)\right]-Vk_Sa_S\left[s_i^L(j)-s_i^S(j)\right]=0 \quad (21)$$
$$Q_L\left[s_i^L(j-1)-s_i^L(j)\right]-Vk_Sa_S\left[s_i^L(j)-s_i^S(j)\right]=0. \quad (22)$$

Catalyst Surface

$$Vk_Sa_S[s_i^L(j)-s_i^S(j)]-V\eta_c w\Phi'[\mathbf{S}(j)]=0. \quad (23)$$

The sensitivity coefficients are defined as (for $j=1,\ \ldots,\ N$)

$$\frac{\partial G_i(j)}{\partial(k_La)}=s_i^G(j) \qquad i=1,\ \ldots,\ m_G$$

$$\frac{\partial L_i(j)}{\partial(k_La)}=s_i^L(j) \qquad i=m_G+1,\ \ldots,\ m_G+m_L$$

$$\frac{\partial S_i(j)}{\partial(k_La)}=s_i^S(j) \qquad i=1,\ \ldots,\ m_G+m_L.$$

For first-order kinetics, as will be encountered in two of the following examples the model and sensitivity equations are linear algebraic equations that can be solved readily by standard techniques.

Screening Method

This procedure recognizes the fact that information regarding the chemistry and kinetics of the reaction may be incomplete and unreliable at the early stage of process devel-

opment but is expected to evolve with time. Let us consider the following scenario. A gas–liquid, liquid–liquid, or gas–liquid–solid catalyst reaction is being tested by the chemist in a laboratory reactor. The reaction (Eq. 1), the phases involved at the chosen operating temperature and pressure, the reactant molar ratio, and the approximate reaction time for the primary reactant are known. An approximate rate expression has been determined. The production rate is specified. The heat of reaction and any other information may or may not be available. The suggested screening procedure, outlined in Figure 7, is described below. Obviously, adjustments are needed if the user's situation is different from this scenario.

1. Choose an appropriate performance index, such as conversion or total cost (Eq. 7).

2. Set up the generic reactor model. Using all known information concerning the reaction, screen the various selection rules listed earlier to select a suitable network model such as those shown in Figure 6. Screen the heuristics listed earlier to select constituent parts for the generic reactor. Alternatively, use a generic model that reflects the laboratory or existing production reactor. Set up the reactor model (Eq. 2) for the generic reactor network created before.

3. Set up the sensitivity model. Identify a set of parameters with respect to which the sensitivity analysis is to be carried out. Set up the sensitivity model (Eqs. 4 to 9).

4. Generate a base case. Screen the various selection rules listed earlier to choose the state of the solid phase. Then, assign base-case values for the phase holdups, with information from the generic phase volume fraction map (Figure 2). Assign base-case values for the mass-transfer coefficients and interfacial areas with information given in Figure 5. From the production rate and the approximate reaction time, estimate a base-case reactor volume. Also assign the base-case values for all remaining parameters in the model, such as recycle ratios, if any. Alternatively, if an existing laboratory or production reactor is used in step 2, use the corresponding parameter values as the base case.

5. Screen the parameters. Determine the predicted reactor performance as well as the sensitivity coefficients for this generic reactor. For the largest sensitivity coefficient, adjust the base-case value for the corresponding parameter to minimize the limitation due to this parameter. This is continued until the performance index is sufficiently high and the reactor is as close to being reaction-controlled as possible. As the parameter values are adjusted, two types of constraints should be recognized. A hard constraint such as ($\epsilon_S + \epsilon_G + \epsilon_L > 1$) is unacceptable and has to be avoided. A soft constraint is one in which the parameter values do not conform to those of a conventional multiphase reactor and is resolved by changing two or more parameter values simultaneously. For example, consider a base case that begins with a dispersed solid phase and that the screening procedure has reached a point where the reactor is as close to being reaction-controlled as possible. The sensitivities indicate that the performance index can be improved by making the catalyst loading correspond to a packed reactor. However, the current particle size on the order of 100 μm is too small for a packed reactor. This is a soft constraint that can be resolved by simultaneously adjusting the value of the particle size as well as the mass-transfer coefficients to reflect the normal range of values for a packed reactor. Despite the fact that the preceding soft constraint violates the heuristic that the pressure drop would be excessive, this seemingly infeasible reactor may give us insights toward the creation of a novel solid-phase structure within the reactor, leading to an entirely new reactor (see previous discussion on monolith solid phase).

6. Identify reactor type and constituent parts. From the phase holdup values at the end of the screening procedure, identify the phase distribution in the reactor using the phase-volume fraction map (Figure 2). From the values of mass-transfer coefficients and interfacial areas, identify the type of gas–liquid interface generating device (Figure 5a). Identify a reactor type corresponding to the preceding parameter values. Note that this may lead to a reactor type not listed in Figure 1, or even a reactor with mutually conflicting parameter values (soft constraints). In such a case back up till the last set of parameter values resulting in a feasible reactor or a new reactor configuration (see step 5).

7. Determine the flow regime. Depending on the state of the solid phase at this stage of the screening procedure, use one of the holdup-flow regime maps (Figures 3a, 3b, or 3c).

8. Check feasibility. To ensure that the chosen reactor and flow regime are consistent with the mass-transfer coefficients, proceed as follows: Depending on the type of the reactor, choose a typical length-to-diameter ratio. From the known gas and liquid flow rates and the phase-volume fractions, calculate the gas and liquid velocities within the reactor. From the conventional-flow regime maps, Figures 8a, 8b, or 8c, determine the flow regime for the phase velocities found earlier (Ramachandran and Chaudhari, 1983; Fan, 1989; and Ng, 1986, respectively). Note that the maps presented in Figure 8 are intended for some specified condi-

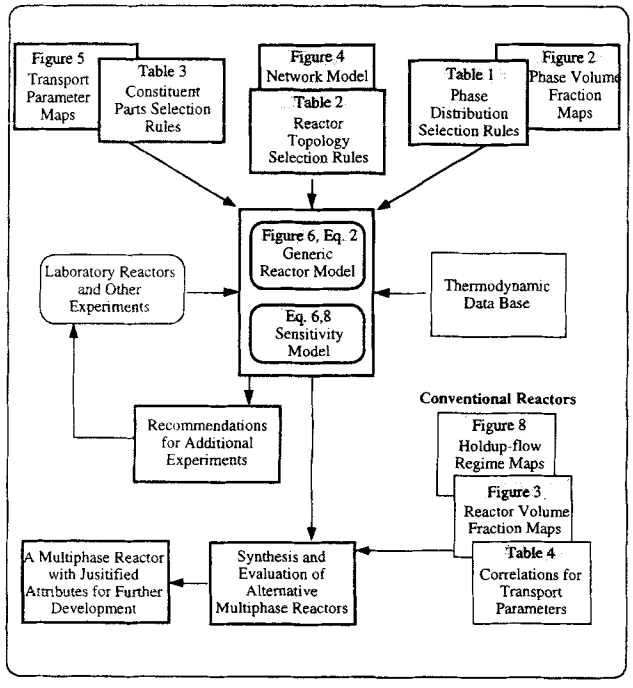

Figure 7. Algorithm for the reactor screening/synthesis procedure.

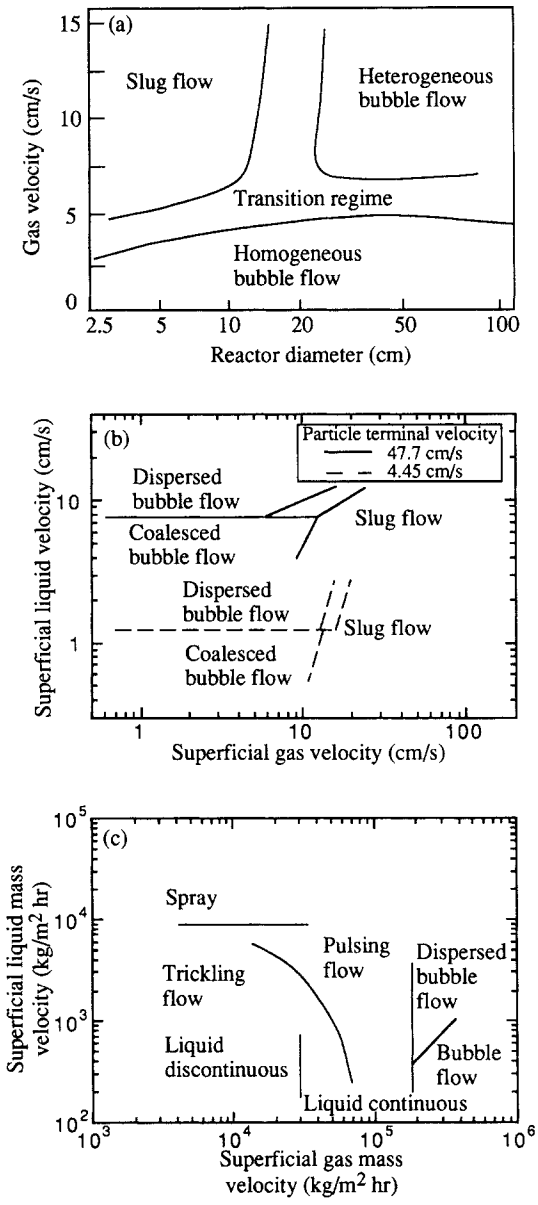

Figure 8. Reactors with (a) dispersed, (b) fluidized and (c) packed solid phase.

tions. If this flow regime does not match with the one determined in step 7, while fixing ϵ_S, adjust the length-to-diameter ratio and, if necessary, ϵ_L and ϵ_G until it does. The mass-transfer coefficients are usually some function of the gas and liquid velocities. Use the correlations in Table 1 to estimate these values. If the mass-transfer coefficients are comparable to those used in the screening procedure, the reactor is a feasible reactor. Care should be exercised because correlations developed from studies on specific systems may not be equally applicable to other systems. If the estimated mass-transfer coefficients are too high or too low, while fixing ϵ_S, again adjust the length-to-diameter ratio and if necessary, ϵ_L and ϵ_G, until the holdups, the flow regime, and the mass-transfer coefficients are all consistent.

The screening procedure is illustrated with the following examples.

Examples

Example 1: Aniline hydrogenation

Consider the hydrogenation of aniline at 10 atm and 130°C over Ni catalyst, supported on clay. Ramachandran and Chaudhari (1980) reported the reaction being carried out in a packed bubble column. The screening procedure proceeds as follows:

Step 1. For a single reaction with a single product, conversion is an adequate performance index, and hence the sensitivity of aniline conversion to the reactor parameters is used in the screening procedure.

Step 2: Generic Model. The reaction has been shown to be first order with respect to H_2, and zero order with respect to aniline. The first-order rate constant k is 51.49 $cm^3/g \cdot s$. The Thiele modulus is based on H_2 as the limiting reactant at the catalyst surface. A simple model such as a network of N stirred tanks in series (Figure 6e) is adequate for the reaction just mentioned. The modeling of the chosen network was illustrated earlier (Eqs. 10 to 19). In this example we only consider a single reaction between the primary reactants.

Step 3: Sensitivity Model. The parameters of interest are k_La, k_Sa_S, k, d_p, w, D_e, and the effectiveness factor η_c. The sensitivity model for the parameter k_La was illustrated earlier (Eqs. 20 to 23). The sensitivity of the performance index (aniline conversion) to the parameter k_La is readily derived as follows, knowing the concentration sensitivity coefficients:

$$\psi(k_La) = -\frac{s^L_{An}(N)}{L^f_{An}}. \tag{24}$$

The sensitivity equations with respect to the other parameters can be set up similarly. The set of the model and sensitivity equations is solved simultaneously for every parameter.

Step 4: Generate Base Case. Since we already have a base case reported by Ramachandran and Chaudhari (1980), start the screening with parameter values close to those of the existing reactor. It is assumed that the required reaction time is available. Since the base case is a packed bubble-column reactor, we start off with a solid holdup of 0.6, and gas and liquid holdups of 0.2 each. The base-case reactor volume can now be calculated using the flow rates, residence times, and the phase holdups. The base-case parameters are summarized in Table 2.

Step 5: Screen Parameters. The sensitivities are calculated for each set of parameter values, and depending on the dominant sensitivities, the parameter values are changed suitably. This process continues until the conversion is no longer very sensitive to any alterable parameter, or until the resulting reactor is infeasible. The possibility of creating a novel reactor, with parameter values that were hitherto considered infeasible, is examined at each stage.

The results are shown in Table 3. The leftmost column shows the iteration number. For each iteration, the numbers above the dashed line indicate the parameter values and the numbers below the dashed line indicate the absolute value of the normalized sensitivity $\bar{\psi}$ of aniline conversion to these parameters. In the first iteration, $\bar{\psi}(k_La)$ with a value of 3.76 is the largest; hence, k_La is increased from 0.02 to 0.1 as signified by a downward pointing arrow in Table 3. This im-

Table 1. Selected Correlations for Hydrodynamic Parameters for Multiphase Reactors*

Bubble column	
Gas–liquid mass-transfer coefficient	
$k_L a = 0.6 \frac{D_L}{d_c^2}\left(\frac{\mu_L}{\rho_L D_L}\right)^{0.5}\left(\frac{g d_c^2 \rho_L}{\sigma_L}\right)^{0.62}\left(\frac{g d_c^3 \rho_L^2}{\mu_L^2}\right)^{0.31} \epsilon_g^{1.1}$	Akita and Yoshida (1973)
Gas–liquid interfacial area	
$a = \frac{1}{3 d_c}\left(\frac{g d_c^2 \rho_L}{\sigma_L}\right)^{0.5}\left(\frac{g d_c^3}{\nu_L}\right)^{0.1} \epsilon_g^{1.13}$	Akita and Yoshida (1974)
Slurry bubble column	
$k_L a$ in the presence of solids	
$\frac{(k_L a)_s}{k_L a} = \left(1 - \frac{\epsilon_S}{0.58}\right)$	Nguyen-Tien et al. (1985)
a in the presence of solids	
$\frac{(a)_s}{a} = \left(\frac{\mu_L}{\mu_{\text{slurry}}}\right)^{0.2}$	Schumpe et al. (1987)
Stirred slurry reactor	
$k_L a$ for low solids gas–liquid systems	
$\frac{k_L a_L d_I^2}{D} = 0.162\left[\frac{N d_I^2 \rho_{sL}}{\mu_{sL}}\right]^{1.5}\left[\frac{\nu_{sL}}{D}\right]^{0.5}\left[\frac{d_I N^2}{g}\right]^{0.19}\left[\frac{\sigma_L}{\mu_{sL} u_g}\right]^{-0.6}\left[\frac{d_1 N}{u_g}\right]^{0.09\sqrt{\sigma_{\text{water}}/\sigma_L}}$	Yagi and Yoshida (1975)
$k_L a$ for slurry systems	
$k_L a_L = 3.07 \times 10^{-3.0} u_g^{0.5\sqrt{\sigma_{\text{water}}/\sigma_L}} \times \sigma_L^{-3.0} \mu_{sL}^{-0.34} (P_T/V_{sL})^{0.75} D_L^{0.5}$	Oguz et al. (1987)
k_{sL} (for $N > N_{\text{crit}}$)	
$\frac{k_{sL} d_p}{D_L} = 2 + 0.55\left(\frac{P_T d_p^4}{\nu_{sL}^3}\right)^{0.25}\left[\frac{\nu_{sL}}{D_L}\right]^{1/3}$	Shah (1991)
Three-phase fluidized bed	
Gas–liquid mass-transfer coefficient	
$k_L a = 1597 u_G^{0.68} u_L^{0.63} d_p^{1.21}$	Chang et al. (1986)
Gas–liquid interfacial area	
$a = 2.08 \times 10^6\, u_G^{0.35} u_L^{0.85} d_p^{0.88}$	Chang et al. (1986)
Solid–liquid mass-transfer coefficient	
$\frac{k_S d_p}{D} = 2 + 0.52\left(\frac{e^{1/3} d_p^{4/3}}{\nu_L}\right)^{0.59}\left(\frac{\mu_L}{\rho_L D}\right)$	Arters and Fan (1988)
Cocurrent packed beds (including trickle beds)	
Gas–liquid mass-transfer coefficient	
$k_L a_p = a_1\left(\frac{E_L D_L}{2.4 \times 10^{-9}}\right)^{a_2}$ where $E_L = \left(\frac{u_L \Delta P_{LG}}{L}\right)\text{W/m}^3$ $E_L > 80$ W/m^3: $a_1 = 0.0173$, $a_2 = 0.5$ $5 < E_L < 100$ W/m^3: $a_1 = 0.0011$, $a_2 = 1.0$ $E_L < 5.0$ W/m^3: $a_1 = 0.008$, $a_2 = 0.0$	Reiss (1967) and Charpentier (1976)
Gas–liquid interfacial area	
$(a_p/a_t) = a_1(\bar{y})^{a_2}$ where $\bar{y} = \frac{\Delta P_{LG}}{L}\frac{\epsilon_p}{a_t}\,Pa$ $\bar{y} > 12$ Pa: $a_1 = 0.25$, $a_2 = 0.5$ $\bar{y} < 12$ Pa: $a_2 = 0.05$, $a_2 = 1.2$	Gianetto et al. (1973) and Charpentier (1976)

*Refer to original reference for definition of terms, and range of applicability.

proves the conversion to 0.274 in iteration 2, and now $\bar{\psi}(\eta_c)$ with a value of 7.63 is the greatest, indicating that internal diffusion controls. But decreasing the catalyst particle size any further leads to a soft constraint. This can be resolved by changing to a dispersed solid state with a smaller particle diameter (0.005 cm), and simultaneously decreasing the catalyst loading (0.02 g/cm^3) to the normal range of values observed in the dispersed solid reactor. This changes $k_s a_s$ to 0.32 s^{-1}. This multiple parameter change is indicated by a double line between iteration 2 and 3. Again, the arrows show

Table 2. Base-Case Parameters for Aniline Hydrogenation Example

V	0.8 m^3	F_{H_2}	0.01 m^3/s
τ_{H_2}	16 s	F^f_{An}	0.0005 m^3/s
τ_{An}	320 s	$C^f_{H_2}$	0.0003 mol/cm^3
ϵ_S	0.6	C^f_{An}	0.0011 mol/cm^3
ϵ_G	0.2	d_p	0.3 cm
ϵ_L	0.2	k_La	0.02 s^{-1}
k	51.49 $cm^3/g \cdot s$	k_sa_s	0.3 s^{-1}

the parameters whose values have been changed by the user during the screening. In iteration 3, $\bar{\psi}(d_p)$ is the highest at 42.9, but the catalyst particle size cannot be decreased much more, without leading to a soft constraint. The effectiveness factor in iteration 3 is much higher at 0.454 because of the small catalyst size, but the high value of $\bar{\psi}(D_e)$, 2.85, indicates that internal diffusion still dominates. However, D_e cannot be changed once the catalyst is fixed, although it clearly shows the incentive of having a catalyst with a higher porosity. $\bar{\psi}(k_La)$ and $\bar{\psi}(w)$ are the other dominant sensitivities. Increasing k_La to 0.4 s^{-1} gives a conversion of 0.61 in the fourth iteration. Since $\bar{\psi}(w)$ is high, some improvement can be obtained by increasing catalyst loading. Thus increasing w to 0.03 g/cm^3 improves the conversion to 0.78, as shown in iteration 5. This is as far as we can go in changing the parameter values.

Step 6: Identify Reactor Type. The preceding set of parameters indicates a dispersed solid phase reactor, with high mass-transfer coefficients, and approximate gas and liquid holdups of 0.3 and 0.6, respectively. This corresponds to a stirred-tank reactor (Figure 1a(iv)) operated at a high rpm, or a jet loop reactor (Figure 1c(iii)), which gives high mass-transfer coefficients.

Step 7: Flow Regime. The gas and liquid holdups used at the end of iteration 5 are 0.3 and 0.67, respectively (not shown in Table 3). This, from the holdup-flow regime map for a reactor with dispersed solid (Figure 3b), corresponds to a churn-turbulent flow regime in the reactor. Note that the gas and liquid holdups along with the length-to-diameter ratio are used as adjustable variables to render the reactor design feasible (see Step 8 of the screening procedure given earlier). They can be adjusted within limits without changing the reactor choice recommended by the screening procedure.

Step 8: Check Feasibility. A length-to-diameter ratio of 1 is chosen for the agitated slurry reactor. The superficial gas velocity can be calculated using the gas flow rate. For the agitated slurry reactor, there is a minimum operating rpm, above which all the catalyst particles are suspended. From the correlation by Zwietering (1958), this is calculated to be about 120 rpm. The Reynolds number in the reactor is given by the following formula

$$Re = \frac{nD^2_{\text{imp}}\,\rho_L}{\mu_L}.$$

Choosing an impeller diameter as one-third of the reactor diameter, Re is found to be 384, which confirms that the flow regime is turbulent, as suggested by the *holdup–flow regime* map (Figure 3). From the correlation of Oguz et al. (1987) for slurry systems (Table 1), a gas–liquid mass-transfer coefficient of 0.4 s^{-1} can be achieved for a power input of 1.5 kW/m^3 (7.5 hp/1,000 gal) of slurry. Thus, all the parameters chosen/recommended by the screening procedure are consistent and the reactor is a feasible one.

A similar feasibility check could be done for a jet loop reactor. The final choice can be made after a more rigorous design and economic evaluation of the two reactor types.

Example 2: Glucose hydrogenation to sorbitol

Consider the Raney-Ni catalyzed hydrogenation of glucose to sorbitol, a versatile chemical intermediate. The screening procedure is described below.

Step 1. Again, the conversion of glucose is chosen as the performance index.

Step 2: Generic Model. Joshi et al. (1988) reported in their review the following Langmuir–Hinshelwood type of rate expression for the preceding reaction:

$$\Phi = \frac{kL_{H_2}L_{Glu}}{1 + KL_{H_2}}. \tag{25}$$

Again, the series of stirred tanks model (Figure 6e) is used for this reaction. The generalized Thiele modulus is based upon H_2 as the limiting reactant at the catalyst surface.

Table 3. Parameter Values and Sensitivity Coefficients of Conversion for Aniline Hydrogenation Example

Iteration	k_La (s^{-1})	k_Sa_S (s^{-1})	k ($cm^3/g \cdot s$)	d_p (cm)	$D_e \times 10^{-6}$ (cm^2/s)	η_c	w (g/cm^3)	Corresponding Conventional Reactor Type
	x_{An}	$\bar{\psi}(k_La)$	$\bar{\psi}(k_Sa_S)$	$\bar{\psi}(k)$	$\bar{\psi}(d_p)$	$\bar{\psi}(D_e)$	$\bar{\psi}(\eta_c)$	$\bar{\psi}(w)$	
1.	0.02	0.3	51.49	0.3	8.35	0.009	0.45		Packed bubble column
	0.086	3.76	0.017	0.013	0.26	0.99	0.767	0.189	
2.	0.10	0.3	51.49	0.3	8.35	0.009	0.45		Packed bubble column
	0.274	1.53	0.168	0.14	0.71	2.85	7.63	0.6	
3.	0.10	0.32	51.49	0.005	8.35	0.454	0.02		Slurry
	0.324	1.45	0.14	0.06	42.9	2.85	0.069	15.9	
4.	0.4	0.32	51.49	0.005	8.35	0.454	0.02		Slurry
	0.615	0.25	0.39	0.17	75.6	5.28	0.19	30.3	
5.	0.4	0.48	51.49	0.005	8.35	0.454	0.03		Slurry
	0.78	0.443	0.309	0.19	97.6	6.74	0.22	25.5	

Table 4. Base-Case Parameters for Glucose Hydrogenation Example

V	16.0 m^3	F_{H_2}	0.02 m^3/s
τ_{H_2}	400 s	F_{Glu}	0.0016 m^3/s
τ_{Glu}	4,950 s	$C^f_{H_2}$	0.006 mol/cm^3
ϵ_S	0.011	C^f_{Glu}	0.001 mol/cm^3
ϵ_G	0.494	d_p	0.005 cm
ϵ_L	0.495	k_La	0.05 s^{-1}
k	$10\left[\frac{cm^3}{mol \cdot s}\frac{\text{g slurry}}{\text{g catalyst}}\right]$	k_Sa_S	0.12 s^{-1}
K (in Eq. 25)	20,000 cm^3/mol		

Step 3: Sensitivity Model. Here, k_La, k_Sa_S, k, d_p, w, D_e, and the effectiveness factor, η_c, are chosen as the parameters of interest.

Step 4: Generate Base Case. The data reported in Joshi et al.'s review are for a bubble-column slurry reactor, and this is chosen as the base case for the screening procedure (Table 4).

Step 5: Screen Parameters. The values of the reactor parameters, as well as the normalized sensitivities $\bar{\psi}$ (absolute values) of the conversion to these parameters are tabulated in Table 5. For the base-case iteration, it is observed that mass transfer is not limiting. $\bar{\psi}(k)$ is high, indicating that the reaction is already kinetically limited. Also, it is not possible to increase the catalyst loading, or decrease catalyst size without pushing the reactor out of the slurry (i.e., dispersed-solid) mode of operation. Hence, in iteration 2 we shift to an entirely different set of reactor parameters, corresponding to a packed state for the solid phase. Simultaneously, the catalyst size and loading are increased to 0.3 cm and 1 g/cm^3, respectively. The glucose conversion is comparable. $\bar{\psi}(\eta_c)$ is the highest at 4.42, implying an internal diffusion control regime. The only way to improve performance now is to increase the catalyst loading, while maintaining the catalyst effectiveness. This can be achieved with the solid phase in a fluidized state. Iteration 3 shows an improved conversion with the catalyst in a fluidized state. Internal diffusion still controls [$\bar{\psi}(\eta_c)$ is high], but the catalyst size cannot be reduced much further, in a fluidized mode of operation. The conversion can be further increased by increasing the catalyst loading to about 25% (v/v), as shown in iteration 4.

Step 6: Identify Reactor Type. These reactor parameters correspond to a three-phase fluidized bed, or an ebulliated bed type of reactor. The design of the fluidized bed is examined in further detail below.

Step 7: Flow Regime. From the particle diameter and the fluid properties, the terminal velocity of the particles is estimated to be 12 cm/s. According to the classification of Fan (1989), the fluidized bed is operating in the expanded mode. From Figure 3b, the regime of operation for gas and liquid holdups of about 0.375 each, is found to be a coalesced bubbly-flow regime. Of course, the continuous and dispersed phases will be decided by the relative flow rates of each phase.

Step 8: Check Feasibility. A length-to-diameter ratio of 5 is chosen for the fluidized bed. The superficial gas and liquid velocities are calculated to be $u_g = 1$ cm/s and $u_l = 0.08$ cm/s. From the flow regime map for fluidized solids (Figure 8b), it is seen that for particles with a terminal velocity of 12 cm/s, the operation would indeed be in the coalesced bubble-flow regime, as found in step 7 of this example. For the preceding gas and liquid velocities, the gas–liquid mass-transfer coefficient is estimated to be about 0.01 s^{-1} (Joshi et al., 1988). This is comparable to the one used in the screening procedure, hence the fluidized bed is a feasible choice for a reactor.

Example 3: Ethoxylation of 1-octanol

1-Octanol ethoxylate, a nonionic surfactant, can be manufactured in a stirred-tank reactor by sparging ethylene oxide into the liquid 1-octanol in the presence of KOH as the catalyst. One of the problems in this reactor system is that the amount of dissolved ethylene oxide in the liquid phase can rise to a level where the formation of undesired byproducts becomes significant. Because of this and other problems, there is a need to consider process alternatives for this gas–liquid system.

Step 1. The conversion of 1-octanol is chosen as the performance index.

Step 2: Generic Model. The exact mechanism of the reaction is as yet unclear, but can be taken to be first order in ethylene oxide concentration. The kinetic data are estimated from the information provided by Di Serio et al. (1996). The series of stirred-tanks models is again chosen to model the preceding system.

Step 3: Sensitivity Model. The parameters of interest are

Table 5. Parameter Values and Sensitivity Coefficients of Conversion for Glucose Hydrogenation Example

Iteration	k_La (s^{-1})	k_Sa_S (s^{-1})	k ($cm^3/g \cdot s$)	d_p (cm)	$D_e \times 10^{-6}$ (cm^2/s)	η_c	w (g/cm^3)	Corresponding Conventional Reactor Type
	x_{Glu}	$\bar{\psi}(k_La)$	$\bar{\psi}(k_Sa_S)$	$\bar{\psi}(k)$	$\bar{\psi}(d_p)$	$\bar{\psi}(D_e)$	$\bar{\psi}(\eta_c)$	$\bar{\psi}(w)$	
1.	0.05	0.12	10.0	0.005	95	0.85	0.05		Slurry bubble column
	0.194	0.003	0.0	1.57	4.995	0.026	1.29	3.16	
2.	0.005	0.22	10.0	0.3	95	0.03	1.0		Trickle bed
	0.136	0.03	0.0	1.14	0.196	0.062	4.42	0.122	
3.	0.005	0.083	10.0	0.08	95	0.105	0.5		Fluidized bed
	0.24	0.17	0.001	1.88	1.28	0.109	7.92	0.39	
4.	0.005	0.122	10.0	0.08	95	0.105	1.0		Fluidized bed
	0.456	0.38	.0009	3.79	2.85	0.24	48.13	0.379	

Table 6. Base-Case Parameters for 1-Octanol Ethoxylation Example

V	0.2 m^3	F_{EO}	0.02 m^3/s
τ_{EO}	4 s	F_{Oct}	0.003 m^3/s
τ_{Oct}	40 s	C^f_{EO}	0.02 mol/cm^3
ϵ_G	0.4	C^f_{Oct}	0.02 mol/cm^3
ϵ_L	0.6	k_La	0.2 s^{-1}
k	2 cm^3/s		

the overall gas–liquid mass-transfer coefficient k_L, the gas–liquid interfacial area a, and the rate constant k.

Step 4: Generate Base Case. The above reaction has been traditionally carried out in a stirred tank reactor which serves as the base case (Table 6).

Step 5: Screen Parameters. Table 7 shows the results of the screening procedure. The base-case iteration clearly shows that the process is controlled by the kinetics. There is no incentive to go for an intensified sparger/mixer such as a venturi ejector to obtain a better k_L and a. However, the second iteration shows that the use of a sparged gas–liquid reactor, without a stirrer, as a means to save on operating cost is not advisable. The conversion is lower than that in the base-case stirred reactor, and the mass transfer and kinetics are equally controlling. Because of the byproduct problem associated with a large amount of dissolved ethylene oxide, it is desirable to keep the liquid holdup to a minimum. The alternative is a spray reactor where 1-octanol is sprayed into the ethylene oxide gas. Iteration 3 shows that due to the poor specific interfacial areas for sprays, the conversion is lesser than in the previous alternatives. Also, the process is now controlled mainly by the gas–liquid interfacial area, with $\bar{\psi}(a)$ being the greatest sensitivity coefficient at 1.28. It is known that the interfacial area is inversely proportional to column height (an $\alpha\ H^{-0.5}$) for spray contactors (Mehta and Sharma, 1970). This leads to a change in the aspect ratio of the reactor. The height-to-diameter ratio is decreased in half and multiple spray nozzles, instead of a single one, are used. Iteration 4 shows that with five spray nozzles, the conversion has improved considerably, and is in fact comparable to that obtained in a stirred tank.

Step 6: Identify Reactor Type. Such a reactor would be like a longitudinal tank, with several spray nozzles along its top and with a continuous ethylene oxide gas feed from the bottom. It is recommended as a candidate for detailed design and economic analysis. Note that such a reactor does not figure among the conventional reactors shown in Figure 1, but has been the commercial reactor of choice (Straneo et al., 1984).

Steps 7 & 8. The reactor operates in the spray flow regime. A separate feasibility study is not necessary for this reactor, since the mass-transfer coefficients chosen are for a liquid spray in gas.

Table 7. Parameter Values and Sensitivity Coefficients of Conversion for Ethoxylation of 1-Octanol Example

Iteration	k_La (s^{-1})	k_L (cm/s)	a (cm^{-1})	k (cm^3/s)	Corresponding Conventional Reactor Type
	x_{Oct}	$\bar{\psi}(k_L)$	$\bar{\psi}(a)$	$\bar{\psi}(k)$	
1.	0.2	0.025	8.0	2.0	Stirred tank
	0.552	0.92	1.15	2.51	
2.	0.1	0.0125	8.0	2.0	Bubble column
	0.306	1.13	0.71	1.45	
3.	0.02	0.02	1.0	2.0	Spray column
	0.065	0.16	1.28	0.32	
4.	0.14	0.02	7.0	2.0	Spray column (multiple nozzles)
	0.42	0.93	1.07	1.93	

Conclusions

The reactor plays a pivotal role in process development. Note only can a good design lower the reactor cost and improve productivity and safety, but also it can influence the reactor effluent stream in such a way that the cost of the downstream separations system can be reduced considerably. As discussed in Lerou and Ng (1996), it is highly desirable to begin reactor synthesis with the laboratory reactor. By using the proposed multiscale approach in which the chemistry, hydrodynamics, transport, and process design are examined concurrently at an early stage of process development, it is more likely for us to come up with a superior process. This is because the design is entirely flexible at this time. The downside is that there is a great deal of uncertainty and missing information about the reaction system.

This article represents our effort to develop a procedure to circumvent this difficulty. Clearly, it is impossible to tackle the whole spectrum of reactions. We limit ourselves to nonfoaming gas–liquid, gas–liquid–solid catalyst, and liquid–liquid reactors discussed in the present article. Other reactor types such as risers and aerosol reactors are not considered. The known conventional multiphase reactors are decomposed into the relevant attributes and constituent parts. These are then reaggregated to form a generic multiphase reactor model. Solution of the model yields predicted reactor performance. More importantly, simultaneous solution of an accompanying sensitivity model provides the possible impact of the various reactor parameters–interfacial area, solubility, kinetics, and others on reactor design despite uncertainty. We do not attempt to come up with a detailed reactor design. Rather, the aim of the procedure is the synthesis of potential reactor types and the identification of parameters for which additional experimental effort is warranted.

Multiphase reactors represent a wide spectrum of problems and issues. Each company or business sector has its own insights and technological knowhow. Thus, the knowledge base presented in this article is not meant to be complete. Rather, the framework is designed in such a way that the user can easily incorporate his or her own experience in the decision-making process.

This screening approach can be extended in a number of directions. The knowledge base can be broadened to include more reactor types. Instead of a single reaction, multiple reactions should be studied so that potential improvements in selectivity can be explored. Heat effect can be considered in a more general generic reactor model. The reactor networks such as those in Figure 6 can be screened more efficiently with mathematical optimization techniques. Most of these efforts are underway.

Acknowledgment

Financial support from the National Environmental Technology Institute and the National Science Foundation (Grant No. 9807101) is gratefully acknowledged. We appreciate the valuable comments by our colleagues at DuPont, Mitsubishi Chemical, Rohm and Haas, and UOP on this screening approach. Specifically, we thank Don Koestler of Rohm and Haas Co. for suggesting the ethoxylation example.

Notation

a = gas-liquid interfacial area per unit volume of reactor, cm^2/cm^3
a_S = solid surface area per unit volume of reactor, cm^2/cm^3
A_i = concentration of ith species taking part in reaction 1
c', c'' = first and second differentials of c with respect to z
C_i = concentration of species i in the phase specified, mol/cm^3
d_p = diameter of (spherical) catalyst particles, cm
D_e = intraparticle diffusion coefficient, cm^2/s
F_i = flow rate of component i, cm^3/s
G_i^f, L_i^f = concentration of species i in the fresh feed of the gas and liquid phase, respectively
H_i = solubility coefficient for species i, $(mol/cm^3)_{gas}/(mol/cm^3)_{liquid}$
k_L = overall gas-liquid mass-transfer coefficient, cm/s
k_S = solid-liquid mass-transfer coefficient, cm/s
n = impeller speed, rps
P = reactor performance index, for example, selectivity, conversion, total cost, and so forth
Q_G, Q_L = actual flow rate of the gas and liquid phase through the cells (= fresh feed + recycle), cm^3/s
$s_i^G(j), s_i^L(j), s_i^S(j)$ = sensitivity with respect to a parameter α of the concentration of the ith species in the jth cell in the gas, liquid, and solid phases, respectively
S_p, V_p = surface area (m^2) and volume (m^3) of a catalyst pellet
V = volume of a single tank in the network, cm^3
V_t = total reactor volume, cm^3
w = catalyst loading per unit volume of reactor, g/cm^3
z = axial direction
$\epsilon_S, \epsilon_L, \epsilon_G$ = solid, liquid, and gas phase holdup in the reactor
Φ = kinetic-rate expression
η_i = catalyst effectiveness factor
μ = viscosity, Pa·s
ν_i = stoichiometric coefficient for species i
ρ = density, g/cm^3
τ_i = residence time of the ith component, s

Subscripts and superscripts

An = aniline
Eo = ethylene oxide
f = feed condition
Glu = glucose
H_2 = hydrogen
l = limiting reactant
Oct = 1-octanol

Literature Cited

Akita, K., and F. Yoshida, "Gas Holdups and Volumetric Mass Transfer Coefficients in Bubble Columns," *Ind. Eng. Chem. Process Des. Dev.*, **12**, 76 (1973).

Akita, K., and F. Yoshida, "Bubble Size, Interfacial Area and Liquid Phase Mass Transfer Coefficient in Bubble Columns," *Ind. Eng. Chem. Process Des. Dev.*, **13**, 84 (1974).

Arters, D. C., and L. S. Fan, "Experimental Methods and Correlation of Solid-Liquid Mass Transfer in Fluidized Beds," *Chem. Eng. Sci.*, **45**, 965 (1990).

Bi, H. T., and J. R. Grace, "Flow Regime Diagrams for Gas-Solid Fluidization and Upward Transport," *Int. J. Multiphase Flow*, **21**, 1229 (1995).

Bischoff, K. B., "Effectiveness Factors for General Reaction Rate Forms," *AIChE J.*, **11**, 351 (1965).

Chang, S. K., Y. Kang, and S. D. Kim, "Mass Transfer in Two and Three Phase Fluidized Beds," *J. Chem. Eng. Jpn.*, **19**, 524 (1986).

Charpentier, J. C., "Recent Progress in Two Phase Gas-Liquid Mass Transfer in Packed Beds," *Chem. Eng. J.*, **11**, 161 (1976).

Cybulski, A., and J. A. Moulijn, "Monoliths in Heterogeneous Catalysis," *Catal. Rev. Sci. Eng.*, **36**, 179 (1994).

Di Serio, M., G. Vairo, P. Iengo, F. Felippone, and E. Santacesaria, "Kinetics of Ethoxylation of 1- and 2-Octanol Catalyzed by KOH," *Ind. Eng. Chem. Res.*, **35**, 3848 (1996).

Doraiswamy, L. K., and M. M. Sharma, *Heterogeneous Reactions*, Vol. 2, Wiley, New York (1984).

Fan, L. S., *Gas-Liquid-Solid Fluidization Engineering*, Butterworths, Boston (1989).

Gianetto, A., V. Specchia, and G. Baldi, "Absorption in Packed Towers with Concurrent Downward High-Velocity Flows—II. Mass Transfer," *AIChE J.*, **19**, 916 (1973).

Gianetto, A., and P. L. Silveston, eds., *Multiphase Chemical Reactors*, Hemisphere, Washington, DC (1986).

Hearfield, F., "Adipic Acid Reactor Developments," *Chem. Eng.*, 625 (1980).

Hildebrandt, D., and D. Glasser, "The Attainable Region and Optimal Reactor Structures," *Chem. Eng. Sci.*, **2**, 2161 (1990).

Hildebrandt, D., and L. T. Biegler, "Synthesis of Chemical Reactor Networks," *Foundations of Computer Aided Process Design*, AIChE Symp. Ser. Vol. 97, No. 304, L. T. Biegler and M. F. Doherty, eds., Amer. Inst. Chem. Eng., New York, p. 52 (1994).

Joshi, J. B., P. V. Shertukde, and S. P. Godbole, "Modelling of Three Phase Sparged Catalytic Reactors," *Rev. Chem. Eng.*, **5**, 1 (1988).

Kingsley, J. P., and K. Roby, U.S. Patent No. 5,523,474 (June 4, 1996).

Kokossis, A. C., and C. A. Floudas, "Optimization of Complex Reactor Networks: I. Isothermal Operation," *Chem. Eng. Sci.*, **45**, 595 (1990).

Kokossis, A. C., and C. A. Floudas, "Optimization of Complex Reactor Networks: II. Nonisothermal Operation," *Chem. Eng. Sci.*, **49**, 7 (1994).

Krishna, R., and S. T. Sie, "Strategies for Multiphase Reactor Selection," *Chem. Eng. Sci.*, **49**, 4029 (1994).

Lerou, J. J., and K. M. Ng, "Chemical Reaction Engineering: A Multiscale Approach to a Multiobjective Task," *Chem. Eng. Sci.*, **51**, 1595 (1996).

Mann, R., "Gas-Liquid Stirred Vessel Mixers," *Chem. Eng. Res. Des.*, **64**, 23 (1986).

Mehta, V. L., and A. Kokossis, "Development of a Novel Multiphase Reactor Using a Systematic Design Procedure," *Comput. Chem. Eng.*, **21**(Suppl.), S325 (1997).

Mehta, K. C., and M. M. Sharma, "Mass Transfer in Spray Columns," *Brit. Chem. Eng.*, **15**, 1556 (1970).

Mills, P. L., P. A. Ramachandran, and R. V. Chaudhari, "Multiphase Chemical Reactors for Fine Chemicals and Pharmaceuticals," *Rev. Chem. Eng.*, **8**, 1 (1992).

Ng, K. M., "A Model for Flow Regime Transitions in Cocurrent Downflow Trickle-Bed Reactors," *AIChE J.*, **32**, 115 (1986).

Ng, K. M., and C. F. Chu, "Reactors, Trickle Bed," *Enclyclopedia of Chemical Processing Design*, Vol. 46, J. J. McKetta, ed., Marcel Dekker, New York, p. 469 (1994).

Nguyen-Tien, K., A. N. Patwari, A. Schumpe, and W. D. Deckwer, "Gas Liquid Mass Transfer in Fluidized Particle Beds," *AIChE J.*, **33**, 328 (1985).

Oguz, H., A. Brehm, and W. D. Deckwer, "Gas Liquid Mass Transfer in Stirred Slurry Reactors," *Recent Trends in Chemical Reaction Engineering*, Vol. II, B. D. Kulkarni, R. A. Mashelkar, and M. M. Sharma, eds., Wiley-Eastern, New Delhi, p. 487 (1987).

Rabitz, H., M. Kramer, and D. Dacol, "Sensitivity Analysis in Chemical Kinetics," *Annual Review of Physical Chemistry*, Vol. 34, S. B. Rabinowitch, M. J. Schurr, and H. L. Strauss, eds., Annual Reviews Inc., Palo Alto, p. 419 (1983).

Rajagopal, S., K. M. Ng, and J. M. Douglas, "Design of Solids Processes—Potash Production," *Ind. Eng. Chem. Res.*, **27**, 2071 (1988).

Ramachandran, P. A., and R. V. Chaudhari, "Predicting Performance of Three Phase Catalytic Reactors," *Chem. Eng.*, **87**, 74 (1980).
Ramachandran, P. A., and R. V. Chaudhari, *Three Phase Catalytic Reactors*, Gordon & Breech, London (1983).
Ramachandran, P. A., and J. M. Smith, "Mixing Cell Method for Design of Trickle-Bed Reactors," *Chem. Eng. J.*, **17**, 91 (1979).
Riess, L. P., "Cocurrent Gas-Liquid Contacting in Packed Columns," *Ind. Eng. Chem. Process Des. Dev.*, **6**, 486 (1967).
Schembecker, G., T. Droge, U. Westhaus, and K. H. Simmrock, "A Heuristic-Numeric Consulting System for the Choice of Chemical Reactors," *Proc. Found. Computer-Aided Proc. Des.*, AIChE Symp. Ser. No. 304, **91**, 336 (1995).
Schumpe, A., A. K. Saxena, and L. K. Fang, "Gas-Liquid Mass Transfer in a Slurry Bubble Column," *Chem. Eng. Sci.*, **42**, 1787 (1987).
Shah, Y. T., *Gas-Liquid-Solid Reactor Design*, McGraw-Hill, New York (1979).
Shah, Y. T., "Design Parameters for Mechanically Agitated Reactors," *Adv. Chem. Eng.*, **17**, 1 (1991).
Straneo, P., C. Maffezzoni, and A. Marchegiano, "Evolution of Ethoxylation Plants for Non-Ionic Surfactant Production," World Surfactants Congress, Munich (1984).
Wen, C. Y., and L. T. Fan, *Models for Flow Systems and Chemical Reactors*, Dekker, New York (1975).
Yagi, H., and F. Yoshida, "Gas Absorption by Newtonian and Non-Newtonian Fluids in Sparged Agitated Vessels," *Ind. Eng. Chem. Process Des. Dev.*, **14**, 488 (1975).
Zwietering, T. N., "Suspending of Solid Particles in Liquid by Agitators," *Chem. Eng. Sci.*, **8**, 244 (1958).

Manuscript received Nov. 17, 1997, and revision received Apr. 6, 1998.